ARTICLE

Line-Profile Analysis of Excitation Spectroscopy in the Even $3p^5(^2P_{1/2})nl'[K']_J(l'=1,3)$ Autoionizing Resonances of Ar

Chun-yan Li[a*], Mei Zhou[a], Zhi-wei He[a], Jin-hong Zhang[a], Yang Chen[b*]

a. College of Science, China Agricultural University, Beijing 100083, China
b. Hefei National Laboratory for Physical Sciences at the Microscale and Department of Chemical Physics, University of Science and Technology of China, Hefei 230026, China

(Dated: Received on January 23, 2016; Accepted on February 23, 2016)

The even-parity autoionizing resonance series $3p^5np'[3/2]_{1,2}$, $3p^5np'[1/2]_1$, and $3p^5nf'[5/2]_3$ of Ar have been investigated exciting from the two metastable states $3p^54s[3/2]_2$ and $3p^54s'[1/2]_0$ in the photon energy range of 32500−35600 cm^{-1} with an experimental bandwidth of ∼0.1 cm^{-1}. The excitation spectra of the even-parity autoionizing resonance series show typical asymmetric line shapes. New level energies, quantum defects, line profile index and resonance widths, resonance lifetime and reduced widths of the autoionizing resonances are derived by a Fano-type line-shape analysis. The line profile index q and the resonance widths Γ are shown to be approximately proportional to the effective principal quantum number n^*. The line separation of the $3p^5np'$ autoionizing resonances is discussed.

Key words: Ar, Autoionizing resonances, Fano-type lineshape

I. INTRODUCTION

The high Rydberg states of rare gases have been a subject of interest to spectroscopists for many years. These ARS are attractive for experimental and theoretical studies because they are rather isolated and their characteristics can be determined with high accuracy. The energy of the Rydberg electron is very sensitive to the potential associated with the ion core and provides information on the polarizability of the many-electron core. The width of the ARS is determined by the interaction of the excited states with the continuum and with the nearby ARS of the same parity and total angular momentum J, these interactions are strongly affected by many-electron correlations. Therefore, studies of ARS allow us to obtain deeper insight into intra-atomic electron dynamics, and a critical comparison between the measured and calculated characteristics of the ARS can provide a crucial test of the theoretical approach [1].

The rare gases (except helium) possess two relatively closely spaced ionization limits corresponding to the $^2P_{3/2}$ and $^2P_{1/2}$ states of the ion core, with the Rydberg series converging to each of these two limits. Since the ionization limits and the autoionizing Rydberg states of the rare gas atoms are of high energies, the spectroscopic investigations starting from their ground states usually requires radiation source in vacuum ultraviolet (VUV) region, where high resolution spectrum is relatively challenging compared to longer wavelength region. Promoting one of the np-subshell (n=2−5) electrons of the rare gases to the next available (n+1)s orbital yields four levels that are built on the $np^5(n+1)s$ configuration, namely $np^5(n+1)s[1/2]_{0,1}$ and $np^5(n+1)s[3/2]_{1,2}$. The $np^5(n+1)s[1/2]_1$ and $np^5(n+1)s[3/2]_1$ levels decay radiatively to the ground state, whereas $np^5(n+1)s[1/2]_0$ and $np^5(n+1)s[3/2]_2$ are metastable [2]. The two metastable levels $3p^54s[3/2]_2$ and $3p^54s'[1/2]_0$ lie at 93143.767 and 94553.665 cm^{-1}, respectively, relative to the argon ground state [3]. This provides an opportunity for excitation to the high lying Rydberg levels via single photon or two photon transitions, which are otherwise not readily accessible from the ground state due to the transition selection rules. Furthermore, these excitation spectra can be obtained with narrow-linewidth laser excitation, thus providing high-resolution studies on the high Rydberg states.

The spectroscopy of high Rydberg states of argon, especially the autoionizing states, has been extensively investigated [3–17]. However, the understanding of even-parity autoionizing Rydberg states of Kr is less comprehensive, and the resolution of the obtained spectra is roughly low. In 1973, Stebbing and Dunning first observed the single photon excitation from the second metastable level $3p^54s'[1/2]_0$ to $3p^5(^2P_{1/2})np'[1/2]_1$ (n=11−20), the even-parity autoionizing states of argon [3]. Later they reported the spectra of single photon excitation to the even parity autoionizing state series $3p^5(^2P_{1/2})np'[3/2]_1$ (n=11−26) and $3p^5(^2P_{1/2})nf'[5/2]_3$ (n=9−15), which are excited from the first metastable level $3p^54f'[3/2]_2$ [4]. Pel-

*Authors to whom correspondence should be addressed. E-mail: chunyanl@cau.edu.cn, yangchen@ustc.edu.cn, Tel.: +86-551-636-06619

larin *et al.* employed the collinear laser spectroscopy with a field ionization detection technique to investigate the even-parity autoionizing resonances below the first ionization limit, $3p^5(^2P_{3/2})np$ (n=12−70)$[1/2]_1$, $[3/2]_2$, $3p^5(^2P_{3/2})np$ (n=12−40)$[3/2]_1$,$[5/2]_{2,3}$, $3p^5(^2P_{3/2})nf$ (n=11−19)$[3/2]_1$, $[5/2]_2$, $[3/2]_2$, $[5/2]_3$ (n=11−38) and $3p^5(^2P_{1/2})np'[1/2]_1$ (n=9, 10), $[3/2]_{1,2}$, nf' (n=7, 8)$[5/2]_{2,3}$ spectra excited from the $3p^54s[3/2]_2$ metastable level [5]. Muhlpfordt and Even observed a ZEKE spectrum of the $3p^5(^2P_{3/2})np$, $3p^5(^2P_{3/2})nf$ and $3p^5(^2P_{1/2})np'$ (n≥15), $3p^5(^2P_{1/2})nf'$(n≥14) Rydberg series converging to the two ionization potential excited from the $3p^54s[3/2]_2$ metastable level, respectively, and reported the ionization limits and quantum defects derived from the line position measurements but did not provide the spectroscopic data [6]. Koeckhoven *et al.* [7] observed four-photon excitation from the ground state and the even parity $3p^5(^2P_{1/2})np'$ (n=11−19) $[1/2]_0$, $[3/2]_1$ and nf' (n=10−15) $[5/2]_2$, $[7/2]_4$ autoionizing Rydberg series, and studied the np' (n=11−13) $[3/2]_1$ and nf' (n=10, 11) $[5/2]_2$ spectra using the line-shape formula derived by Ueda [18]. Peter *et al.* reported the experimental and theoretical investigation of even $mp^5(^2P_{1/2})np'$ (m=2−5) autoionizing resonances of rare gas atoms and provided Fano lineshape analysis of argon np' (n=13, 14) $[1/2]_1$, $[3/2]_2$ [8]. Lee *et al.* reported some np' and nf' autoionizing series by stepwise excitations from instant intermediate states with lasers and synchrotron radiation [9].

The studies on odd-parity Rydberg states have been more extensive. Wu *et al.* [10] reported high resolution photoelectron spectrum of argon odd-parity $3p^5(^2P_{1/2})12s'$, $10d'$ autoionizing states excited from the ground state, and analyzed it using the line-shape formula derived by Ueda [18]. Klar *et al.* observed the high resolution two-photon excitation spectra of the metastable Ar* and reported odd-parity $3p^5(^2P_{1/2})ns'$ (n=18−25) J=0, 1 levels [11]. Koeckhoven *et al.* reported three-photon excitation spectra from the ground state and the odd-parity $3p^5(^2P_{1/2})ns'$ (n=11−34) $[1/2]_1$, nd' (n=9−21) $[3/2]_1$, ng' (n=9−21) $[7/2]_3$ autoionizing Rydberg states [12]. Landais *et al.* [13] observed the $3p^5(^2P_{1/2})ns'$ (n=11−34) $[1/2]_{0,1}$ autoionizing levels using two step optical excitation from the $3p^54s[3/2]_2$ metastable level, and analyzed the spectra for n=11−25. Piracha *et al.* [14] reported the odd parity $3p^3ns$, nd, $3p^3nd'$ (n=6−8) series excited from the $3p^54s[3/2]_2$ metastable level and $3p^3ns'$ (n=10−30) $[1/2]_0$, nd' (n=15−29) $[3/2]_2$ series excited from the $3p^54s'[1/2]_0$ metastable level using single-color two-photon excitation. Weber *et al.* [15, 16] reported the high resolution odd-parity $3p^3(^2P_{3/2})ns$, nd (n=13−90) J=2, 3, and ng (n=13−70) J=4 Rydberg spectra together with the low lying $3p^3(^2P_{1/2})$ nd' (n=10−14), and $3p^3(^2P_{1/2})$ ng' (n=7−9) autoionizing states, and carried out multichannel quantum defect analysis of the J=2, 3, 4 levels. Recently, Zheng *et al.* [17] reported the odd parity $3p^3(^2P_{3/2})ns$ (J=1, 2), nd (J=0−4) Rydberg series and $3p^3(^2P_{1/2})$ ns' (J=0, 1, n=7−10), nd' (J=1−3, n=5−9) autoionizing states spectra excited from the two metastable levels $3p^54s[3/2]_2$ and $3p^54s'[1/2]_0$ populated in a pulsed DC discharge.

Although many experiments have been carried out for the Ar autoionizing Rydberg states including $3p^5np'$ and $3p^5nf'$, few high-resolution spectroscopic studies and very few line profile parameters are available. We recently reported the systematic experiment study of the autoionizing $3p^5np'$ and $3p^5nf'$ resonance series of argon by using pulsed DC discharge along with single UV photon excitation and the TOF-MS technique [19]. In that work, the metastable $Ar^*(3p^54s[3/2]_2$ and $3p^54s'[1/2]_0)$ atoms were produced by a pulsed high-voltage DC discharge and are then excited to the even-parity autoionizing resonances series $3p^5np'[3/2]_{1,2}$, $3p^5np'[1/2]_1$, and $3p^5nf'[5/2]_3$ by a pulsed UV laser radiation with a narrow bandwidth of ∼0.1 cm^{-1}. These autoionizing resonance states subsequently decay to Ar^+ ions, which are detected using the time-of-flight (TOF) mass spectrometry. The excitation spectra of the autoionizing resonance series are recorded in the form of the Ar^+ ion intensities as a function of excitation UV laser radiation. The high-resolution excitation spectra show typical asymmetric line shapes. In the present work, the high-resolution excitation spectra are fitted using Fano line-shape formula, and new results for the resonance energies, quantum defects, line profile indexes, resonance widths, resonance lifetimes and reduced widths are derived from the observed resonance spectra.

II. EXPERIMENTS

The experiment was conducted in a laser ionization mass spectrometer described elsewhere [19]. Briefly, the photoionization experimental apparatus includes the metastable Ar* atoms source and the ion detection system. The metastable Ar* atoms were produced by a DC discharge of a mixture of 5% SF_6 in Ar at a stagnation pressure of 5 atms. A pulsed high voltage of about 2 kV was supplied to the electrodes producing a discharge in the area of the orifices of the copper electrodes. The supersonic beam after the DC discharge was collimated by a skimmer (ϕ=3 mm) and entered into the photoexcitation and photoionization chamber. The photoionization chamber was maintained at typical pressures of $\sim10^{-4}$ and $<10^{-5}$ Pa, respectively, with and without the operation of the beam. A Nd:YAG laser (Spectra Physics, GCR-190) pumping a dye laser (Lumonics, HT-500) was used as the light source (pulse duration of UV radiation is about 8 ns, energy per UV pulse is typically 1.0 mJ). The dye laser output was frequency doubled with a second harmonic generator (Lumonics, HT-1000) and then focused perpendicularly on the metastable Ar* beam by a 250 mm focal length

DOI:10.1063/1674-0068/29/cjcp1601012

lens. Ions generated via autoionizing process at the ionization zone were introduced and accelerated to the flight tube of the TOF mass spectrometer and then detected by micro-channel plates (MCP). The mass resolved ion signal from the MCP was amplified by an amplifier (Stanford Research System, SR445) and averaged by a digital oscilloscope (Tektronix, TDS3032B) or a computer data acquisition system. A multi-channel delay pulsed generator was used to control the relative time delays among the nozzle, the laser, and the DC discharge.

The mass resolved photoexcitation spectra were obtained by setting the corresponding time gate to monitor the arrival of m/z=40 ($^{40}Ar^+$) ions and recording the ion signals as a function of laser wavelength. No attempt was made to normalize the spectral intensity with respect to the laser power. The typical scan speed of the dye laser was 0.001 nm/s at a 10 Hz laser repetition. Calibration of the laser wavelength was achieved by a wavelength meter (Coherent).

III. RESULTS AND DISCUSSION

The excited levels of the rare gas are designated in the $j_c l[K]_J$ coupling scheme [20–23], in which the orbital angular momentum l of the excited electron is weakly coupled to the total angular momentum j_c (3/2 or 1/2) of the $np^5_{j_c}$ ionic core to yield the resultant quantum angular momentum K. K is then weakly coupled with the spin s of the excited electron giving total angular momentum J. The propensity rules for electric dipole transitions in the jK-coupling scheme are: ΔJ=0, ±1; ΔK=0, ±1; and Δj=0. These rules are well observed, and wherever ΔJ=ΔK=+Δl, the transition lines possess higher intensity. However, the Δj=0 rule is not followed strictly, since transitions with a change of the ionic core are also often observed.

The autoionization states are excited from the two metastable Ar* states by one photon resonance transition. Based on the transition rules and the threshold for direct photoionization from the Ar* metastable to the autoionizing resonance series, the observed series of the autoionizing structures as reported [19] are identified as $3p^5(^2P_{1/2})4s'[1/2]_0 \xrightarrow{h\nu} 3p^5(^2P_{1/2})np'[3/2]_1$, $3p^5(^2P_{3/2})4s[3/2]_2 \xrightarrow{h\nu} 3p^5(^2P_{1/2})np'[3/2]_{1,2},[1/2]_1$, and $3p^5(^2P_{3/2})4s[3/2]_2 \xrightarrow{h\nu} 3p^5(^2P_{1/2})nf'[5/2]_3$, respectively. Since the autoionizing resonances lie between the two ionization potentials in the $^2P_{3/2}$ continuum, the perturbation arising from interactions among the resonance series having the same parity and J, and the perturbation arising from interactions with the $^2P_{3/2}$ continuum, are complex. The perturbation influences the Rydberg electron of Ar and manifests on the variation of the principal quantum defects. The width of the spectrum peak reflects the lifetime of the resonance. The experimental results show that, as the principal quantum number n increases, the quantum defects of the given series increase whereas the widths of the autoionizing peaks corresponding to the given series decrease. This is expected because the interaction with the $^2P_{3/2}$ continuum is greater near threshold. The lifetime of the autoionizing resonances will be discussed below.

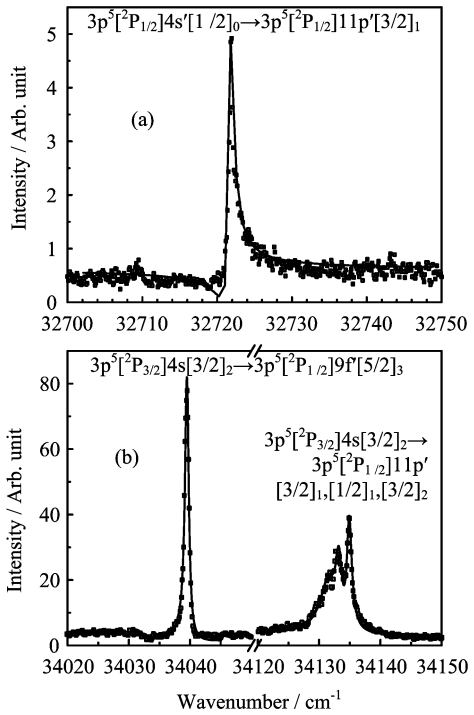

FIG. 1 The partially expanded spectra of the autoionizing resonances. (a) The experimental data (dots) and Fano line profile fitting curve of the autoionizing line $3p^5 11p'[3/2]_1$ excited from $3p^5 4s'[1/2]_0$. (b) The experimental data (dots) and Fano line profile fitting curve of autoionizing lines $3p^5 11p'[3/2]_{1,2}$, $[1/2]_1$ and $3p^5 9f'[5/2]_3$ excited from $3p^5 4s[3/2]_2$.

A. Line-profile analysis of the $3p^5 np'$ and $3p^5 nf'$ autoionizing resonances

The line profiles for all the observed transitions between 32500 and 35600 cm^{-1}, *i.e.*, $3p^5(^2P_{1/2})4s'[1/2]_0 \xrightarrow{h\nu} 3p^5(^2P_{1/2})np'[3/2]_1$, $3p^5(^2P_{3/2})4s[3/2]_2 \xrightarrow{h\nu} 3p^5(^2P_{1/2})np'[3/2]_{1,2}$, $[1/2]_1$, and $3p^5(^2P_{3/2})4s[3/2]_2 \xrightarrow{h\nu} 3p^5(^2P_{1/2})nf'[5/2]_3$, show typical asymmetric line shapes, as seen in Fig.1. A theoretical treatment of these line shapes due to autoionizing transitions has been carried out by Fano *et al.* [24, 25]. For an isolated autoionizing state, the photoion production cross section can be described by the Fano formula:

$$\sigma(E) = \sigma_b + \sigma_a \frac{(q+\varepsilon)^2}{1+\varepsilon^2} \quad (1)$$

$$\varepsilon = \frac{E - E_r}{\Gamma/2} \quad (2)$$

DOI:10.1063/1674-0068/29/cjcp1601012

TABLE I Parameters obtained by line profile analysis for the $4s'[1/2]_0$ (94553.665 cm^{-1})→$3p^5np'[3/2]_1$, $4s[3/2]_2$ (93143.767 cm^{-1})→$3p^5np'[3/2]_1$, $[3/2]_2$, $[1/2]_1$ (E_r, Γ, and Γ_r in cm^{-1}, and τ in 10^{-12}s).

	$3p^5np'[3/2]_1$←$4s'[1/2]_0$						$3p^5np'[3/2]_1$←$4s[3/2]_2$					
n	E_r	q	Γ	τ	δ	Γ_r	E_r[b]	q	Γ	τ	δ	Γ_r
11	127275.345	2.87±0.04	0.81±0.02	6.57	1.690	652	127275.337	−9.9±3.6	2.95±0.28	1.80	1.690	2381
12	127508.965	2.65±0.06	0.74±0.04	7.18	1.690	810	127509.017	−8.4±2.0	2.81±0.19	1.89	1.690	3080
13	127683.845	2.55±0.06	0.60±0.03	8.88	1.688	866	127683.677	−12.2±5.0	2.79±0.16	1.90	1.689	4037
14	127817.315	2.57±0.06	0.45±0.03	11.90	1.689	832	127817.537	−10.0±5.5	2.30±0.49	2.31	1.688	4293
15	127922.765	2.32±0.06	0.52±0.03	10.17	1.681	1233	127921.967	−7.4±2.6	1.75±0.14	3.03	1.690	4126
16	128005.315	2.06±0.05	0.44±0.03	12.09	1.693	1286	128005.467	−11.5±3.7	1.27±0.07	4.18	1.691	3721
17	128073.215	2.18±0.07	0.38±0.03	14.04	1.690	1356	128073.237	−11.6±7.3	1.15±0.11	4.62	1.690	4127
18	128128.495	1.97±0.08	0.29±0.03	18.18	1.698	1265	128128.867	−9.8±5.6	1.00±0.12	5.31	1.690	4339
19	128174.815	1.43±0.07	0.31±0.04	17.24	1.698	1595	128174.717	−6.5±3.2	0.44±0.11	12.07	1.701	2278
20	128213.665	1.81±0.07	0.32±0.03	16.64	1.702	1954	128213.477	−5.8±3.2	0.30±0.17	17.70	1.707	1836
21	128246.865	1.43±0.09	0.27±0.04	20.03	1.698	1906	128246.657	−4.5±6.0	0.28±0.31	18.96	1.705	2011
22	128275.015	1.46±0.10	0.25±0.04	21.49	1.704	2065	128274.887	−4.4±5.8	0.28±0.25	18.96	1.708	2340
23	128299.335	1.38±0.12	0.16±0.03	33.60	1.708	1525	128299.527	−7.3±18.0	0.40±0.27	13.27	1.700	3865
	$3p^5np'[3/2]_2$←$4s[3/2]_2$						$3p^5np'[1/2]_1$←$4s[3/2]_2$					
n	E_r	q	Γ	τ	δ	Γ_r	E_r[b]	q	Γ	τ	δ	Γ_r
11	127278.767	−10.5±1.6	0.95±0.06	5.59	1.677	770	127277.017	−11.8±0.3	1.28±0.11	4.15	1.684	1035
12	127511.617	−10.7±1.6	0.97±0.04	5.47	1.677	1067	127510.217	−10.8±3.1	1.00±0.09	5.31	1.684	1098
13	127685.677	−15.4±4.7	0.88±0.05	6.03	1.676	1278	127684.587	−12.9±7.8	1.02±0.13	5.20	1.683	1478
					1.668	*700*					*1.675*	*3600*
14	127819.007	−14.0±4.2	0.80±0.05	6.64	1.675	1498	127818.067	−10.2±7.6	0.70±0.12	7.58	1.683	1308
					1.668	*700*					*1.675*	*3600*
15	127923.167	−10.6±3.9	0.78±0.05	6.81	1.677	1845	127922.617	−8.0±1.6	0.51±0.08	10.41	1.683	1204
16	128006.417	−13.8±5.9	0.62±0.04	8.56	1.678	1821	128005.967	−9.6±4.3	0.26±0.05	20.42	1.684	763
17	128073.937	−14.0±9.6	0.45±0.05	11.80	1.679	1618	128073.527	−9.0±10.3	0.35±0.11	15.17	1.685	1257
18	128129.717	−12.8±8.5	0.45±0.04	11.80	1.674	1958	128129.367	−9.0±3.2	0.30±0.10	17.70	1.680	1304
19	128175.757	−13.8±3.6	0.29±0.02	18.31	1.676	1508	128175.347	−11.3±3.2	0.42±0.05	12.64	1.686	2180
20	128214.437	−10.3±4.5	0.45±0.06	11.80	1.68	2767	128213.967	−8.3±5.8	0.28±0.12	18.96	1.693	1718
21	128247.527	−10.0±8.9	0.40±0.11	13.27	1.676	2886	128247.137	−7.9±7.0	0.25±0.16	21.24	1.689	1800
22	128275.676	−11.5±4.8	0.32±0.04	16.59	1.678	2686	128275.267	−7.2±6.5	0.30±0.13	17.70	1.694	2512
23	128300.027	−9.3±16.7	0.31±0.13	17.13	1.678	3005	128299.847	−7.6±13.5	0.30±0.28	17.70	1.686	2905

Note: The italic data in n=13, 14 are experiment results from Ref.[8].

Here σ_b represents the portion of the cross section describing transitions to the continuum that do not interact with the quasi-bound (autoionizing) states, and σ_a is the resonant portion of the cross section. E is the observed term energy, E_r is the resonance energy, q is the line profile index, and Γ is the resonance width.

Fano profile has been fitted to the present data, providing values of E_r, q, Γ for each of the observed transitions (listed in Table I−III). The partially expanded spectra of the autoionizing resonances are shown in Fig.1 as an example to illustrate the comparison of the Fano profile curve fitting to the experimental spectra. The smooth curves represent fits to the experimental spectra (dots). Figure 1(a) shows the experimental data and Fano line profile fitting curve of the autoionizing line $3p^511p'[3/2]_1$ excited from the metastable level $3p^54s'[1/2]_0$. Figure 1(b) shows the experimental data and Fano line profile fitting curve of the autoionizing lines $3p^511p'[3/2]_{1,2}$, $[1/2]_1$ and $3p^59f'[5/2]_3$ excited from the first metastable level $3p^54s[3/2]_2$. For $n\geq24$, the three states of the np' series, $3p^5(^2P_{1/2})np'[3/2]_2$, $[3/2]_1$, $[1/2]_1$, are not distinguishable; their q and Γ parameters are the sum of the three states and their values are listed respectively in Table II. Note that most of the line profile analysis of the $3p^5np'[3/2]_{1,2}$, $[1/2]_1$ and $3p^5nf'[5/2]_3$ autoionizing resonances are reported for the first time. For members of a Rydberg series, the reduced width Γ_r is defined as $\Gamma_r=\Gamma_n n^{*3}$, where $n^*=n-\delta$ is the effective quantum number, and the corresponding quantum defect δ and effective quantum number n^* are

DOI:10.1063/1674-0068/29/cjcp1601012

TABLE II Parameters obtained by line profile analysis for the $3p^5np'\leftarrow 4s[3/2]_2$[a] (93143.767 cm^{-1}) ($n\geq 24$).

n	E_r[b]/cm^{-1}	q	Γ/cm^{-1}	$\tau/10^{-12}$s	δ	Γ_r/cm^{-1}
24	128321.097	10.07±0.88	0.69±0.02	7.69	1.682	7670
25	128339.217	−10.90±0.16	0.60±0.03	8.85	1.703	7587
26	128355.487	−11.13±0.12	0.56±0.02	9.48	1.705	8030
27	128369.847	−9.02±0.12	0.52±0.02	10.21	1.708	8413
28	128382.627	−10.16±0.20	0.49±0.04	10.83	1.710	8904
29	128393.907	−6.42±0.20	0.63±0.07	8.43	1.724	12784
30	128404.077	−7.34±0.15	0.53±0.03	10.02	1.732	11972
31	128413.247	−7.97±0.19	0.45±0.04	11.80	1.738	11275
32	128421.467	−7.14±0.24	0.48±0.05	11.06	1.751	13285
33	128428.847	−6.38±0.18	0.43±0.04	12.35	1.775	13091
34	128435.657	−4.98±0.28	0.43±0.08	12.35	1.786	14375
35	128441.967	−4.45±0.35	0.33±0.08	16.09	1.779	12099

[a] Three states of the np' series are not distinguished when $n\geq 24$, so the data of the parameter q, Γ, and $n^{*3}\Gamma$ are the sum of the three states of $3p^5np'[3/2]_1$, $[3/2]_2$, $[1/2]_1$.

TABLE III Parameters obtained by line profile analysis for the $3p^5nf'[5/2]_3\leftarrow 4s[3/2]_2$ (93143.767 cm^{-1}).

n	E_r^*/cm^{-1}	q	Γ/cm^{-1}	$\tau/10^{-12}$s	δ	Γ_r/cm^{-1}
9	127183.267	−17.93±0.13	0.76±0.02	6.95	0.011	555
10	127441.727	−17.53±0.16	0.68±0.02	7.76	0.011	682
11	127632.647	−16.53±0.23	0.58±0.03	9.08	0.011	776
12	127778.127	−15.32±0.20	0.50±0.02	10.62	0.010	862
13	127890.867	−14.46±0.20	0.46±0.02	11.44	0.012	1017
14	127980.417	−13.01±0.20	0.43±0.02	12.26	0.014	1185
15	128052.717	−13.25±0.32	0.41±0.03	12.98	0.015	1376
16	128111.947	−11.34±0.34	0.39±0.04	13.54	0.015	1601
17	128161.117	−9.76±0.41	0.38±0.05	13.93	0.013	1868

calculated using the Rydberg formula. The obtained values of the reduced width Γ_r are listed in Tables I−III. The lifetime of the upper state against autoionization τ is readily determined from $\tau=\hbar/\Gamma$, and the values of τ are also included in Tables I−III.

As shown from the data listed in the Tables I−III, the absolute value of line profile index q decreases when n increases. This indicates that the profile symmetry for high autoionizing resonances is more asymmetric, *i.e.*, the portion of the cross section describing transition to the continuum possesses more percentage in the transition from the lower electronic level to higher upper autoionizing resonances. The present results show that the resonance width Γ value decreases as the principal quantum number n increases, which directly reflects the decrease in natural linewidths of the np' and nf' resonances and increase of their lifetimes. This is expected because the interaction of the resonance states with the $^2P_{3/2}$ continuum is greater (thus faster autoionization) when the resonances are near the threshold, where the density of the continuum is higher. The lifetimes of the $3p^5np'[3/2]_1$ autoionizing resonance series change significantly with a ratio 5−7 between the observed highest and lowest levels, whereas the lifetimes of the $3p^5np'[3/2]_2$, $[1/2]_1$ and $nf'[5/2]_3$ change with a ratio 2−4.

It is noted that the q and Γ value vary with the effective quantum number n (shown in Fig.2). In order to see the relations for the q and Γ value *vs.* the effective quantum number n^*, the q and Γ as function of n^* are plotted and shown in Fig.2. From these figures, the empirical results are obtained: the q is proportional to the effective quantum number n^* for the autoionizing resonance series, and $\ln\Gamma$ is approximately proportional to $\ln n^*$.

B. Line separation of the $3p^5np'$ autoionizing resonances

In the jK coupling scheme, the energy difference depends only on the Slater exchange integral G^1 resulting from the electrostatic interaction, the fine structure interval is expected to be proportional to $1/n^{*3}$ [1, 13, 23]. The experimental fine

DOI:10.1063/1674-0068/29/cjcp1601012

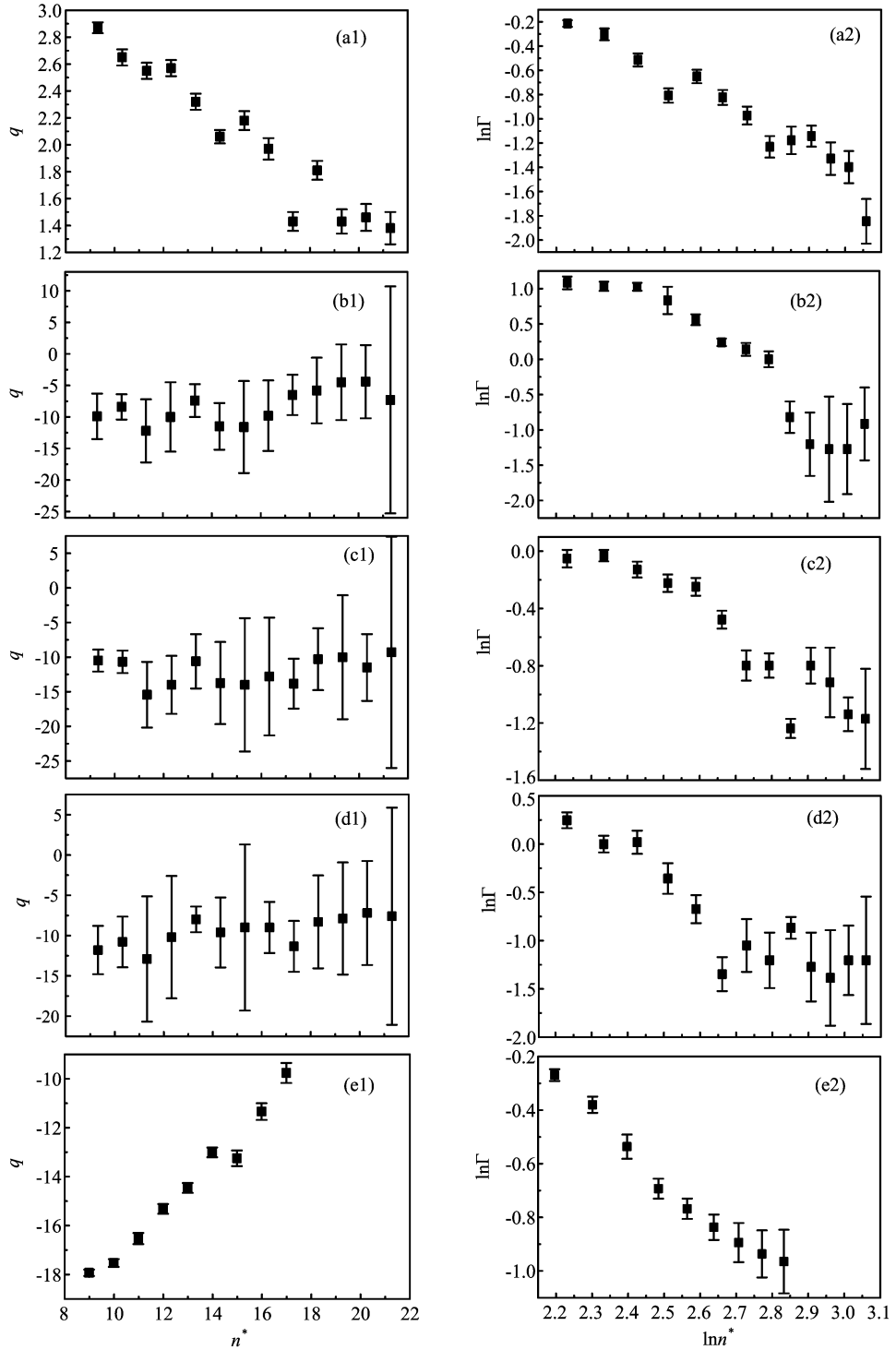

FIG. 2 Autoionizing line profile index q and resonance width Γ of (a) $3p^5np'[3/2]_1$ series excited from $4s'[1/2]_0$, (b) $3p^5np'[3/2]_1$ series excited from $4s[3/2]_2$, (c) $3p^5np'[3/2]_2$ series excited from $4s[3/2]_2$, (d) $3p^5np'[1/2]_1$ series excited from $4s[3/2]_2$, (e) $3p^5nf'[5/2]_3$ series excited from $4s[3/2]_2$ plotted against effective quantum number n^*.

structure interval data of the $3p^5np'$ autoionizing resonances are plotted as a function of averaged effective quantum number n^* as $\ln n^*$ and shown in Fig.3. For $n<15$ and $n>18$, the line has a slope of -2.829 ± 0.219 (difference between $3p^5np'[3/2]_2$ and $3p^5np'[3/2]_1$), -2.619 ± 0.482 (between $3p^5np'[1/2]_1$ and $3p^5np'[3/2]_1$), and -2.774 ± 0.258 (between $3p^5np'[3/2]_2$ and $3p^5np'[1/2]_1$), respectively, compa-

DOI:10.1063/1674-0068/29/cjcp1601012

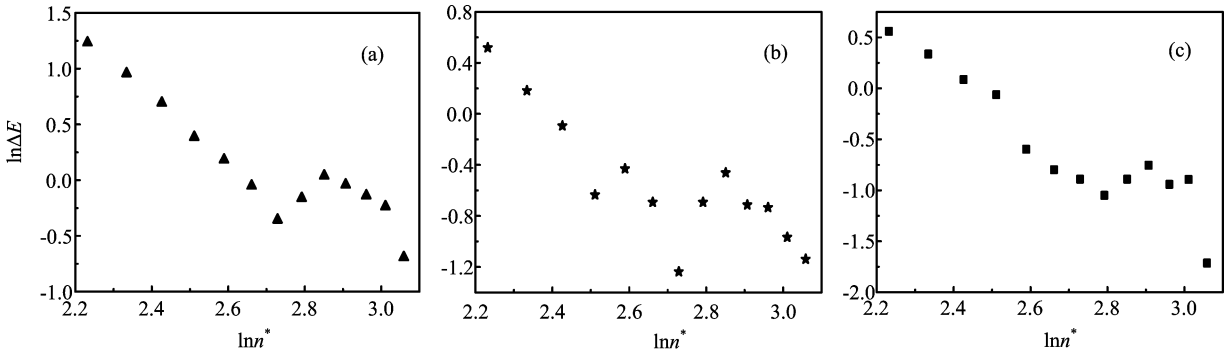

FIG. 3 Energy difference of the $3p^5np'$ autoionizing resonances energy levels plotted against $\ln n^*$.

rable to the expected slope of -3. The results are in good agreement with the theoretical estimate of the fine structure interval. It is noted that the fine structure interval does not follow the expected $1/n^{*3}$ behavior for n=16, 17. This might suggest that the resonance positions of the observed series for n=16, 17 are irregular. Since the signal-to-noise is quite good for the n=16, 17 lines, the derived positions are reliable. One possibility for the irregular line positions of n=16, 17 is that other transitions nearby perturb these states.

IV. CONCLUSION

We have carried out the experiment study of the autoionizing $3p^5np'$ and $3p^5nf'$ resonance series of argon by using pulsed DC discharge along with single UV photon excitation and the TOF-MS technique. The Fano line profile analysis of the excitation spectra is carried out and the Fano parameters of the systematic autoionizing series are reported. The line profile index q and resonance widths Γ are shown to be approximately proportional to the effective principal quantum number n^*. The line separation of the $3p^5np'$ autoionizing resonances is also discussed.

V. ACKNOWLEDGMENTS

This work is supported by the Beijing Higher Education Young Elite Teacher Project (No.YETP0324) and the National Natural Science Foundation of China (No.21403297, No.61474142, and No.11474355).

[1] I. D. Petrov, V. L. Sukhorukov, and H. Hotop, J. Phys. B **36**, 119 (2003).
[2] N. E. Small-Warren and Lue-Yung Chow Chiu, Phys. Rev. A **11**, 1777 (1975).
[3] R. F. Stebbing and F. B. Dunning, Phys. Rev. A **8**, 665 (1973).
[4] F. B. Dunning and R. F. Stebbing, Phys. Rev. A **9**, 2378 (1974).
[5] M. Pellarin, J. L. Vialle, M. Carre, J. Lerme, and M. Aymer, J. Phys. B **21**, 3833 (1988).
[6] A. Muhlpfordt and U. Even, J. Chem. Phys. **103**, 4427 (1995).
[7] S. M. Koeckhoven, W. J. Burma, and C. A. de Lange, Phys. Rev. A **51**, 1097 (1995).
[8] T. Peter, T. Halfmann, U. Even, A. Wunnenberg, I. D. Petrov,V. L. Sukhorukov, and H. Hoptop, J. Phys. B **38**, S51 (2005).
[9] Y. Y. Lee, T. Y. Dung, R. M. Hsieh, J. Y. Yuh, Y. F. Song, G. H. Ho, T. P. Huang, W. C. Pan, I. C. Chen, S. Y. Tu, A. H. Kung, and L. C. Lee, Phys. Rev. A **78**, 022509 (2008).
[10] J. Z. Wu, S. B. Whitfield, C. D. Caldwell, M. O. Krause, P. van der Meulen, and A. Fahlman, Phys. Rev. A **42**, 1350 (1990).
[11] D. Klar, K. Harth, J. Ganz, T. Kraft, M. W. Ruf, H. Hotop, V. Tsemekhman, and M. Y. Amusia, Z. Phys. D **23**, 101 (1992).
[12] S. M. Koeckhoven, W. J. Burma, and C. A. de Lange, Phys. Rev. A **49**, 3322 (1994).
[13] J. Landais, M. Huet, H. Kucal, and T. Dohnalik, J. Phys. B **28**, 2395 (1995).
[14] N. K. Piracha, M. A. Baig, S. A. Khan, and B. Suleman, J. Phys. B **30**, 1151 (1997).
[15] J. M. Weber, K. Ueda, D. Klar, J. Kreil, M. W. Ruf, and H. Hotop, J. Phys. B **32**, 2381 (1999).
[16] J. Bommels, J. M. Weber, A. Gopalan, N. Herschbach, E. Leber, A. Schramm, K. Ueda, M. W. Ruf, and H. Hotop, J. Phys. B **32**, 2399 (1999).
[17] X. F. Zheng, T. T. Wang, and Y. Chen, Chin. J. Atom. Mol. Phys. **21**, 605 (2004).
[18] K. Ueda, Phys. Rev. A **35**, 2484 (1987).
[19] C. Y. Li, Z. W. He, T. T. Wang, J. F. Zhen, Y. Chen, and J. S. Zhang, Chin. J. Chem. Phys. **26**, 259 (2013).
[20] G. Racah, Phys. Rev. **62**, 438 (1942).
[21] I. I. Sobelman, *Atomic Spectra and Radiative Transitions*, Berlin Heidelberg: Springer-Verlag (1979).
[22] R. D. Cowan, *The Theory of Atomic Structure and Spectra*, Berkeley: University of California Press, (1981).
[23] R. D. Knight and L. G. Wang, J. Opt. Soc. Am. B **3**, 1673 (1986).
[24] U. Fano, Phys. Rev. **124**, 1866 (1961).
[25] U. Fano and J. W. Cooper, Phys. Rev. A **137**, 1364 (1965).

DOI:10.1063/1674-0068/29/cjcp1601012